UC-92

SAND85-2027
Unlimited Distribution
November, 1985

FIELD TEST OF DRAG REDUCING AGENTS IN A THREE-INCH PIPELINE AT THE WEST HACKBERRY, LOUISIANA SPR SITE

by

Thomas E. Hinkebein
SPH Geotechnical Division
Sandia National Laboratories
Albuquerque, New Mexico 87185

ABSTRACT

A flow test of seven drag reducing agents (DRAs) was carried out at the Strategic Petroleum Reserve (SPR) site at West Hackberry, Louisiana. A 3-inch pipeline was operated with DRA addition, at controlled concentrations, to flowing brine while the fluid flow rate and the pressure drop were continuously monitored. The fluid flow rates were controlled so that the wall shear stress in the 3-inch pipeline approximated the wall shear stress in the 36-inch brine disposal pipeline at the West Hackberry SPR site. Two classes of materials were tested: a guar and six polyacrylamide DRAs. These materials were tested at concentrations up to 19 parts per million (ppm). The polyacrylamide DRAs all have a higher level of activity than the guar, but demonstrate a susceptibility to pipe roughness that the guar did not. The six polyacrylamide DRAs showed maximum friction factor reductions at 19 ppm between 27% and 44%. The maximum friction factor reduction for the guar DRA was 9%. The performances of all DRAs were functions of concentration and were fit by a power law model. The performance of the polyacrylamides was proportional to approximately the 0.9 power of concentration while that of the guar was proportional to the 1.5 power. At the test flow condition, the improvement observed in these drag reduction experiments should be equivalent to flow improvement in the 36-inch pipeline.

TABLE OF CONTENTS

LIST OF FIGURES

LIST OF TABLES

INTRODUCTION

The Department of Energy requested that Sandia National Laboratories perform an evaluation of the use of drag reducing agents (DRAs) in brine pipelines within the SPR. The first phase of this evaluation was a laboratory investigation in which thirty materials were screened at Southwest Research Institute[1]. Subsequently, a field test was carried out in a 3-inch diameter pipeline at West Hackberry, Louisiana, where seven polymeric DRAs were tested. These materials were the most effective among those tested in the first phase of testing. This second phase of testing is the subject of this report. In order to satisfy legal requirements, these materials are referred to only by number in this report.

When DRAs are added to flowing fluid, the turbulence level in the fluid is reduced. This lower turbulence may be manifest in a smaller pressure drop at the same flow rate or in increased flow at the same pressure drop. The advantages of adding drag reducing agents to the brine disposal pipeline system within the SPR are one or more of the following. The system may have greater economy in pumping, increased reliability in the pumping network, or reduced leaching time due to increased flow rates.

This report consists of a description of the experiment in the 3-inch pipeline, the results of the testing, and the analysis of the results.

EXPERIMENT - EQUIPMENT

The pipeline used in this investigation was a 3-inch diameter steel pipe shown schematically in Figure 1. Brine was withdrawn from the 36-inch brine disposal pipeline (WH-36-BR-10026) at West Hackberry, passed through the test section, and was discharged into a 24-inch brine disposal pipeline (WH-24-BR-1000-D). WH-36-BR-10026 was operated at 787 psi during the testing period and WH-24-BR-1000-D was operated at 0 psi. The test pipeline was a 3-inch, class 600 ANSI, schedule 80 pipe (2.9-inch inside diameter).

Within the test section, brine flow was controlled by partially opening two, 2-inch globe type, hand control valves, each with a maximum C_V of 34.5 gal/psi. The flow rate was measured by a 2-inch Halliburton turbine flow meter in conjunction with a Halliburton Model MP-1 Flow Analyzer. Differential pressure measurements were taken between two pressure taps at the centerline location, located 75 feet apart on the side of the pipe.

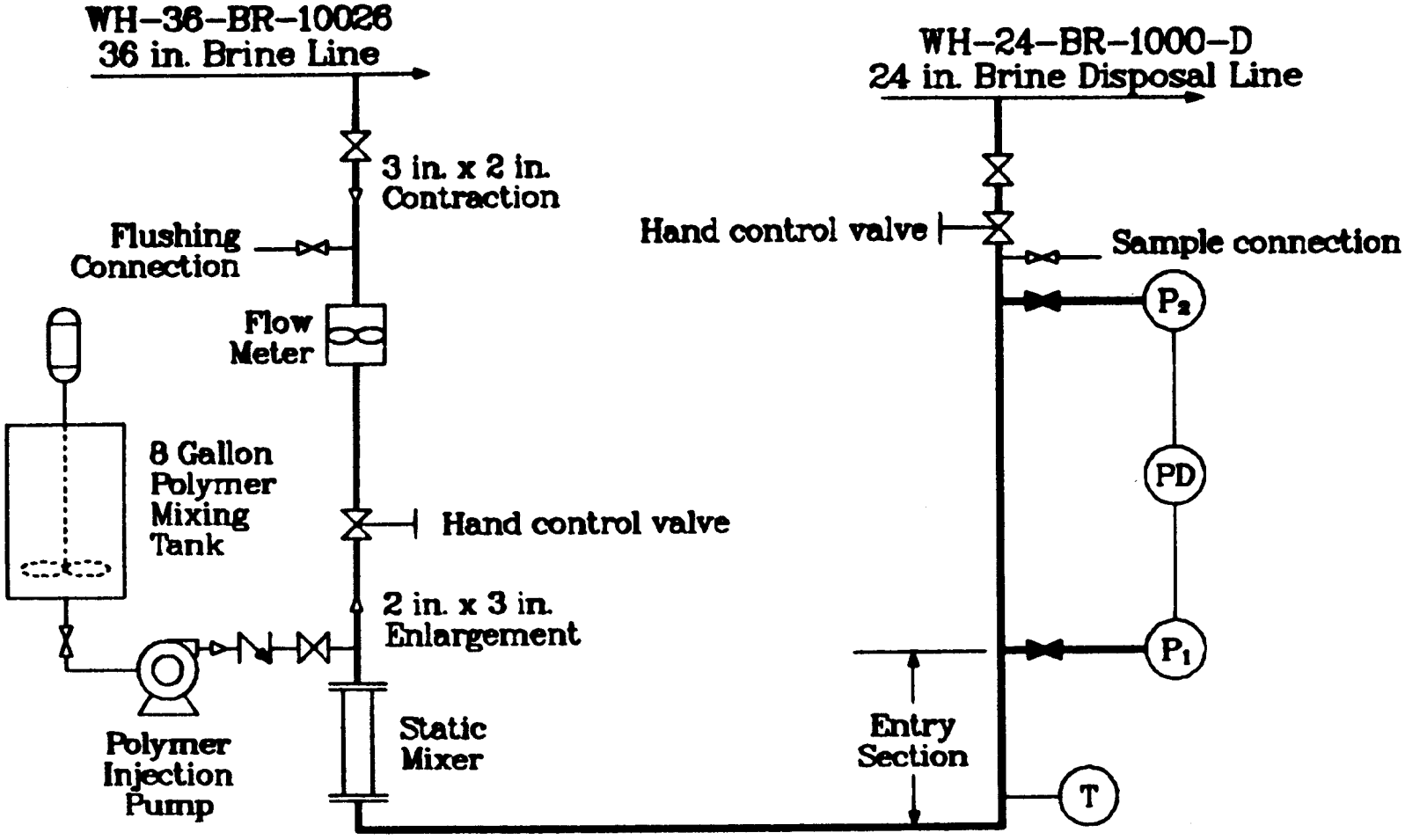

Figure 1. Schematic of polymer test pipeline.

Gauge pressure measurements were also made at Pl. The pressure drop along the test section was measured by a Sensotec Model Z/3749 wet/wet differential pressure transducer (with a range of ±10 psid). This transducer produces a voltage proportional to the differential pressure. The voltage was measured with a Thermo-Systems Model 1076 Volt Meter which has a lo-second time constant. The pipeline gauge pressure was determined by a Viatran Model 218-15 gauge pressure transducer (with a range of 0 to 2000 psig). Upstream of the P_1 pressure tap, a 35-foot section of 3-inch pipe acted as an entry section. Within this entry section, liquid temperature was measured at location "T" with a Yellow Springs Instruments' PT-139AP RTD connected to a Fluke 2180A RTD Digital Thermometer.

DRAs were prepared in a batch mode in an 8-gallon mixing tank and then metered into the pipeline with a MilRoyal Model C positive displacement pump. This pump may be adjusted to give any flow rate between 0 and 49 gal/hr at 1050 psi. Downstream of the DRA addition point, a Komax Systems Motionless Mixer with a minimal 5 psi pressure drop provided for homogeneous mixing of the DRA with the brine stream while assuring that DRA degradation was not a factor in these experiments.

EXPERIMENT - PROCEDURE

For these experiments, it was desirable to measure the reduction in pressure drop following the addition of DRA while holding the flow rate constant. To accomplish this, a constant flow rate was established by manually adjusting both hand control valves. Through a proper adjustment of both valves, the overall gauge pressure in the test pipeline was also controlled. A baseline differential pressure was then measured using the Sensotec transducer and the Thermo-Systems volt meter. When the volt meter time constant was set at 10 seconds, the meter output would reach a constant value within one minute. This constant value was then recorded.

The polymer injection pump was then started and DRA was injected at a constant rate into the pipeline. The DRA mixed with the fluid in the pipeline and the differential pressure transducer asymptotically approached a reduced voltage level over the next minute. This new voltage was recorded. When DRA was added, the overall flow rate remained constant and no adjustment of the hand control valves was required.

Three nominal flow rates were used in evaluating each of the DRAs. These flow rates were chosen to allow scaling of the results to the 36-inch brine disposal pipeline. The scaling laws

developed in SAND85-0045 [2] require a correspondence between the wall shear stresses for each application. Accordingly, flow rates of 100, 150, and 200 gpm were chosen for this study.

DRA preparation was done as a batch operation. Individual formulations were prepared in fresh water according to manufacturers specifications. Each polymer solution wa6 mixed in an 8-gallon tank for one hour before being metered into the brine stream. DRA addition rate6 were selected to bracket the useful concentration range of each material. This concentration range was determined by the desire to achieve an approximate 20% reduction in pressure drop at constant flow rate. Additionally, the maximum flow rate of the polymer injection pump limited DRA concentration to approximately 19 ppm. Three different concentration level6 were investigated for each material.

TEST RESULTS

The brine used in these tests was a NaCl brine with a specific gravity of 1.176. Total suspended solids of 104 mg/l were present and the pH was 6.51. Approximately 1000 mg/l of divalent calcium was present in the brine. The brine temperature varied between 87.7 and 89.5°F. Under these conditions the brine density was 73.4 lb/ft^3 and the brine behaved a6 a Newtonian fluid with a viscosity of $9.15x10^{-4}$ lb/ft-sec.

The results of the tests with each DRA are reported in Tables 1 through 7. At each concentration and flow rate condition, differential pressure was measured in the 75-foot test section both at the baseline condition (no DRA) and with DRA added. After each test the baseline was reverified to assure no residual effects or baseline drift. The order of presentation of the data is chronological.

Table 1.
Experimental Pressure Drop and Flow Rate Data for Material 1.
The brine temperature was 89.5°F.

Concentration (ppm)	Flow Rate (gpm)	Static Pressure (psi)	Differential Pressure No DRA Added (psi)	Differential Pressure DRA Added (psi)	Differential Pressure Reduction (%)
19.1	200.5	557.2	6.740	6.140	8.9
19.3	150.0	618.4	3.892	3.600	7.5
19.1	100.9	730.0	1.894	1.772	6.4
10.1	200.5	567.2	6.662	6.460	3.0
10.0	150.0	659.6	3.820	3.680	3.7
9.57	100.9	717.6	1.874	1.838	1.9
0.92	200.5	624.0	6.684	6.684	0.0
0.92	150.0	657.6	3.862	3.878	0.0
0.91	100.9	716.0	1.884	1.884	0.0

Table 2.
Experimental Pressure Drop and Flow Rate Data for Material 2.
The brine temperature was 88.6°F.

Concentration (ppm)	Flow Rate (gpm)	Static Pressure (psi)	Differential Pressure No DRA Added (psi)	Differential Pressure DRA Added (psi)	Differential Pressure Reduction (%)
19.2	200.0	504.0	6.500	4.560	29.8
19.3	150.0	530.0	3.720	2.390	35.8
19.2	100.0	674.0	1.640	0.990	39.6
3.19	200.0	562.0	6.498	6.100	6.1
3.24	150.0	614.0	3.716	3.360	5.5
3.22	100.0	678.0	1.644	1.452	11.7
1.72	200.0	689.6	6.480	6.280	3.1
1.70	150.0	712.0	3.706	3.462	6.6
1.68	100.0	767.2	1.634	1.484	9.2

Table 3.
Experimental Pressure Drop and Flow Rate Data for Material 3.
The brine temperature was 89.8°F.

Concentration (ppm)	Flow Rate (gpm)	Static Pressure (psi)	Differential Pressure No DRA Added (psi)	Differential Pressure DRA Added (psi)	Differential Pressure Reduction (%)
19.2	200.0	428.8	6.446	5.240	18.7
19.3	150.0	489.2	3.770	2.884	23.5
19.2	100.0	412.0	1.716	1.250	27.2
3.19	200.0	398.0	6.690	6.500	2.8
3.24	150.0	476.0	3.710	3.570	3.8
3.22	100.0	388.0	1.684	1.622	3.7
1.72	200.0	421.6	6.850	6.860	0.0
1.70	150.0	445.2	3.800	3.810	0.0
1.68	100.0	382.0	1.760	1.760	0.0

Table 4.
Experimental Pressure Drop and Flow Rate Data for Material 4.
The brine temperature was 89.7°F.

Concentration (ppm)	Flow Rate (gpm)	Static Pressure (psi)	Differential Pressure No DRA Added (psi)	Differential Pressure DRA Added (psi)	Differential Pressure Reduction (%)
19.2	200.0	446.0	6.504	4.580	29.6
19.3	150.0	466.0	3.722	2.302	38.2
19.2	100.0	378.0	1.684	0.944	43.9
3.19	200.0	400.8	6.480	6.110	5.7
3.24	150.0	421.6	3.744	3.462	7.5
3.22	100.0	361.6	1.680	1.502	10.6
1.61	200.0	413.2	6.510	6.390	1.8
1.58	150.0	464.0	3.726	3.598	3.4
1.54	100.0	360.8	1.710	1.540	9.9

Table 5.
Experimental Pressure Drop and Flow Rate Data for Material 5.
The brine temperature was 88.6°F.

Concentration (ppm)	Flow Rate (gpm)	Static Pressure (psi)	Differential Pressure No DRA Added (psi)	Differential Pressure DRA Added (psi)	Differential Pressure Reduction (%)
19.2	200.0	382.0	6.466	4.668	2'1.8
19.3	150.0	578.8	3.724	2.540	31.8
19.2	100.0	378.8	1.70%	1.220	28.3
3.19	200.0	384.0	6.564	6.140	6.5
3.24	150.0	479.6	3.740	3.520	5.9
3.22	100.0	372.0	1.664	1.570	5.6
1.61	200.0	38fl.8	6.520	6.440	1.2
1.58	150.0	544.0	3.682	3.604	2.1
1.54	100.0	372.8	1.660	1.642	1.1

Table 6.

Experimental Pressure Drop and Flow Rate Data for Material 6.
The brine temperature was 88.4°F.

Concentration (ppm)	Flow Rate (gpm)	Static Pressure (psi)	Differential Pressure No DRA Added (psi)	Differential Pressure DRA Added (psi)	Differential Pressure Reduction (%)
19.2	200.0	388.8	6.556	4.780	27.1
19.3	150.0	595.2	3.710	2.584	30.4
19.2	100.0	405.6	1.668	1.180	29.3
3.19	200.0	336.0	6.510	6.110	6.1
3.24	150.0	621.2	3.636	3.360	7.6
3.22	100.0	388.0	1.644	1.514	7.9
1.61	200.0	404.0	6.520	6.380	2.1
1.58	150.0	492.0	3.680	3.580	2.7
1.54	100.0	380.0	1.636	1.602	2.1

Table 7.

Experimental Pressure Drop and Flow Rate Data for Material 7. The brine temperature was 87.7°F.

Concentration (ppm)	Flow Rate (gpm)	Static Pressure (psi)	Differential Pressure No DRA Added (psi)	Differential Pressure DRA Added (psi)	Differential Pressure Reduction (%)
19.2	200.0	388.0	6.550	4.380	33.1
19.3	lso.o	521.2	3.898	2.400	38.4
19.2	100.0	390.0	1.650	1.000	39.4
3.19	200.0	400.0	6.560	6.040	7.9
3.24	150.0	522.0	3.780	3.400	10.1
3.22	100.0	380.8	1.704	1.502	11.9
1.61	200.0	350.4	6.550	6.328	3.4
1.58	150.0	552.0	3.730	3.570	4.3
1.54	100.0	368.0	1.670	1.604	4.0

DATA REDUCTION METHODOLOGY

The performance of drag reducing agents is readily described on differential Prandtl-Karman coordinates[3]. Prandtl-Karman (P-K) coordinates have $1/\sqrt{f}$ as the ordinate and $\log(Re\sqrt{f})$ as the abscissa, where f is the Fanning friction factor, and Re is the Reynolds number. Differential P-K coordinates look only at the improvement,

$$\frac{1}{\sqrt{f_p}} - \frac{1}{\sqrt{f_s}}$$

as a function of

$$\log (Re\sqrt{f}/d).$$

The subscripts p and s refer to the friction factor observed in the brine with and without DRA, respectively. The abscissa is normalized with respect to d, the pipe diameter, so that the abscissa is directly proportional to the logarithm of the wall shear stress. Turbulent flow plots as zero on the ordinate. Since DRA performance is directly related to the wall shear stress, the results expressed on these coordinates are applicable to any diameter pipeline [2].

Although a more complete description of the performance of DRAs in brine is given in SAND85-0045 [2], a brief summary of

their performance is presented here. Turbulent flow of a fluid containing a drag reducing agent can be divided into three major flow regions as illustrated in Figure 2. First, on P-K coordinates, there is a regime of Newtonian turbulence, Region I, in which the fluid behaves as if there were no DRA present. Second, there is a regime above a critical wall shear stress, Region II, where the friction factor with DRA present is less than the corresponding Newtonian friction factor and the differential P-K values linearly increase with increasing shear stress. Third, at higher wall shear stresses the flow becomes completely turbulent as the wall roughness decreases the effectiveness of the DRA. In this regime, Region III, the friction factor approaches a constant value which is still less than the completely turbulent flow of a non-drag reduced solution. On P-K coordinates, the DRA performance curve in Region III goes through a maximum and then decreases to a steady-state value. The wall shear stress at which transition to completely rough flow occurs is determined solely by the pipe roughness and the polymer itself[4]. Both the 3-inch test loop and the 36-inch pipeline operate in the completely turbulent polymeric flow regime. Hence, the data obtained in this experiment allow a projection of the performance of DRAs in the 36-inch brine disposal pipeline when plotted on P-K coordinates. The actual performance of DRAs in the 36-inch pipeline will also depend on the difference in pipe roughness between the 3-inch and 36-inch pipes. The greater roughness in the 36-inch pipe may reduce the actual improvement observed, but this effect must be quantified experimentally.

DATA REDUCTION

The data presented in Tables 1 through 7 are converted to Reynolds number and Fanning friction factors. The Reynolds number is defined as

$$Re = \frac{dV\rho}{\mu} ,$$

where

Re = Reynolds number,
V = Average fluid velocity,
ρ = Fluid density,
μ = Fluid static viscosity, and
d = Pipe diameter.

The Fanning friction factor is defined as

$$f = \frac{g_c d\Delta P}{2\rho V^2 L} ,$$

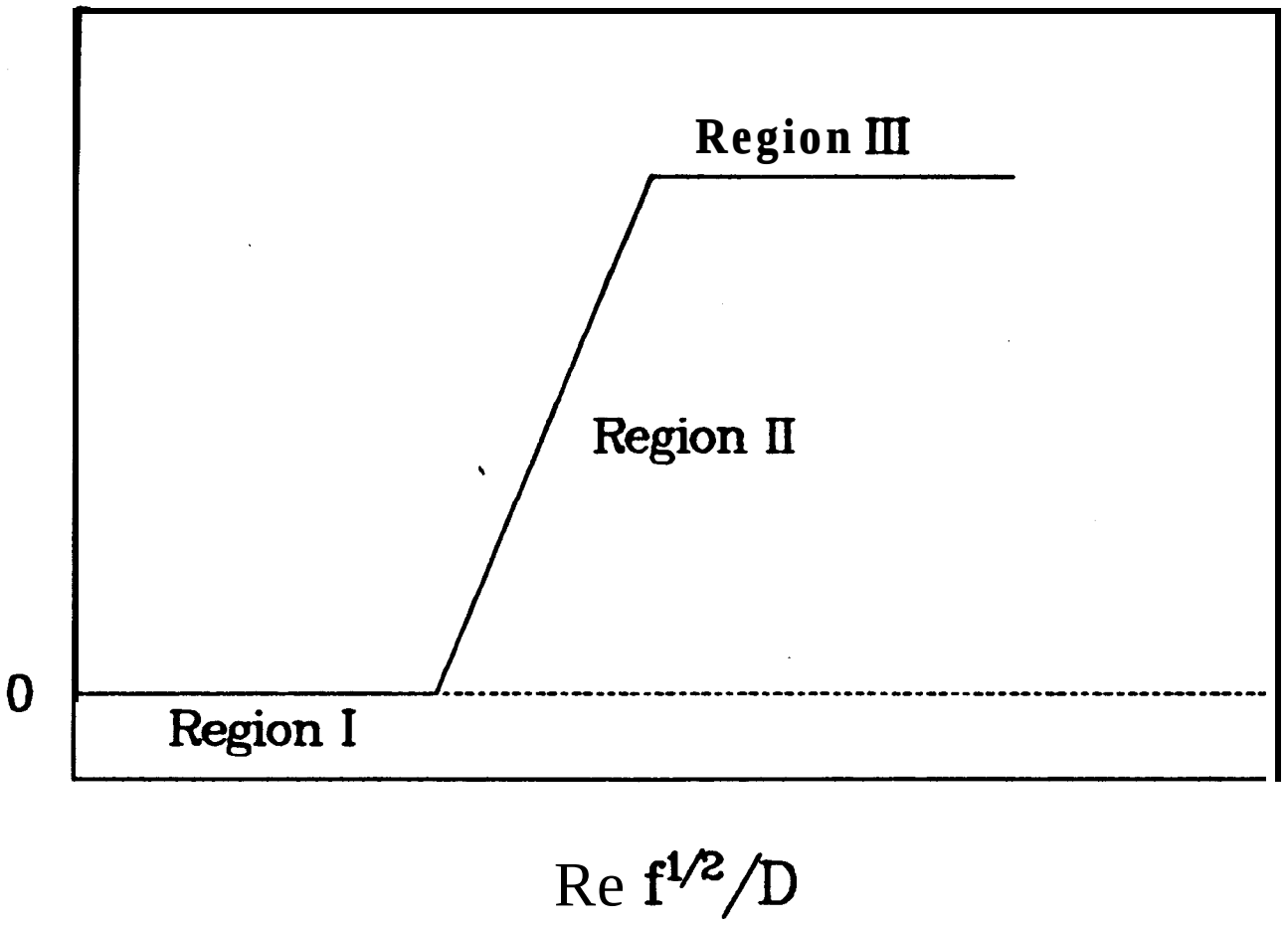

Figure 2 Generalized relationship between Reynolds Number and ↗□✳♍♦✳□■ **factor on differential P–K coordinates. The three regions of turbulent flow with DRAs in the fluid are shown.**

where

f = Fanning friction factor,
g_c = Gravitational constant,
ΔP = Pressure drop along the length of pipe, and
L = Length of pipe.

The data presented in Tables 1 through 7 are plotted on differential P-K coordinates in Figures 3 through 9.

ERROR ANALYSIS

Before looking at the results of these experiments, first consider the error involved in these measurements. A standard analysis of error was performed on all of the baseline differential pressure measurements. At the 90% probability level, these measurements were accurate to within ±2.2%. At the same time, the Halliburton flow meter had a specified accuracy of ±0.5%. When taken together in a propagation of error analysis, these individual inaccuracies lead to an overall error in

$$\frac{1}{\sqrt{f_p}} \qquad \frac{1}{\sqrt{f_s}}$$

of approximately ±0.4 as shown in Figures 3 through 9.

It is felt, however, that this measure of inaccuracy may be excessive. A probable cause of the majority of the error in differential pressure measurements was thermal drift within the transducer. The measurement procedure we used called for a direct comparison of the differential pressure with and without DRA to be made within a few minute time period. In this short time it is felt that thermal drift would be minimal. Nonetheless, the inaccuracy in the results where differential pressure reduction was small may be large.

The polymer delivery pump also had some error associated with its operation. The accuracy of this pump was determined in replications of a calibration curve. It was found that at high delivery rates, corresponding to the 3-19 ppm concentration of DRA in the brine. the injection rate was within ±1-5% of the average flow rate. Higher accuracy was observed at the highest injection rate. At l-2 ppm concentration of DRA in the brine,

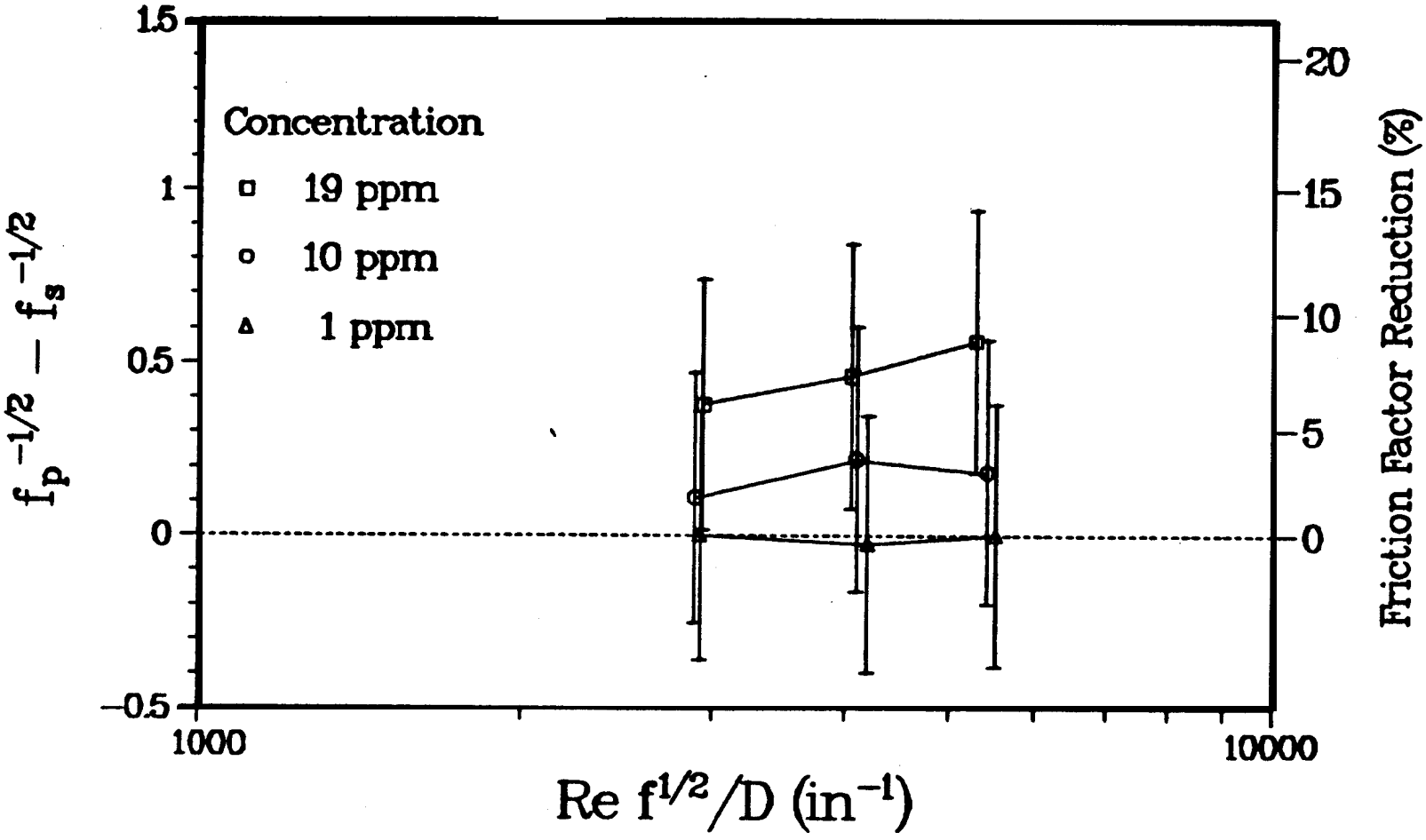

Figure 3. Relationship between Reynolds Number and friction factor on differential P–K coordinates for material #1. For reference purposes an approximate nonlinear coordinate is constructed on the right hand ordinate. It shows the percentage reduction in friction factor, or, correspondingly, the percentage reduction in pressure drop at constant flow.

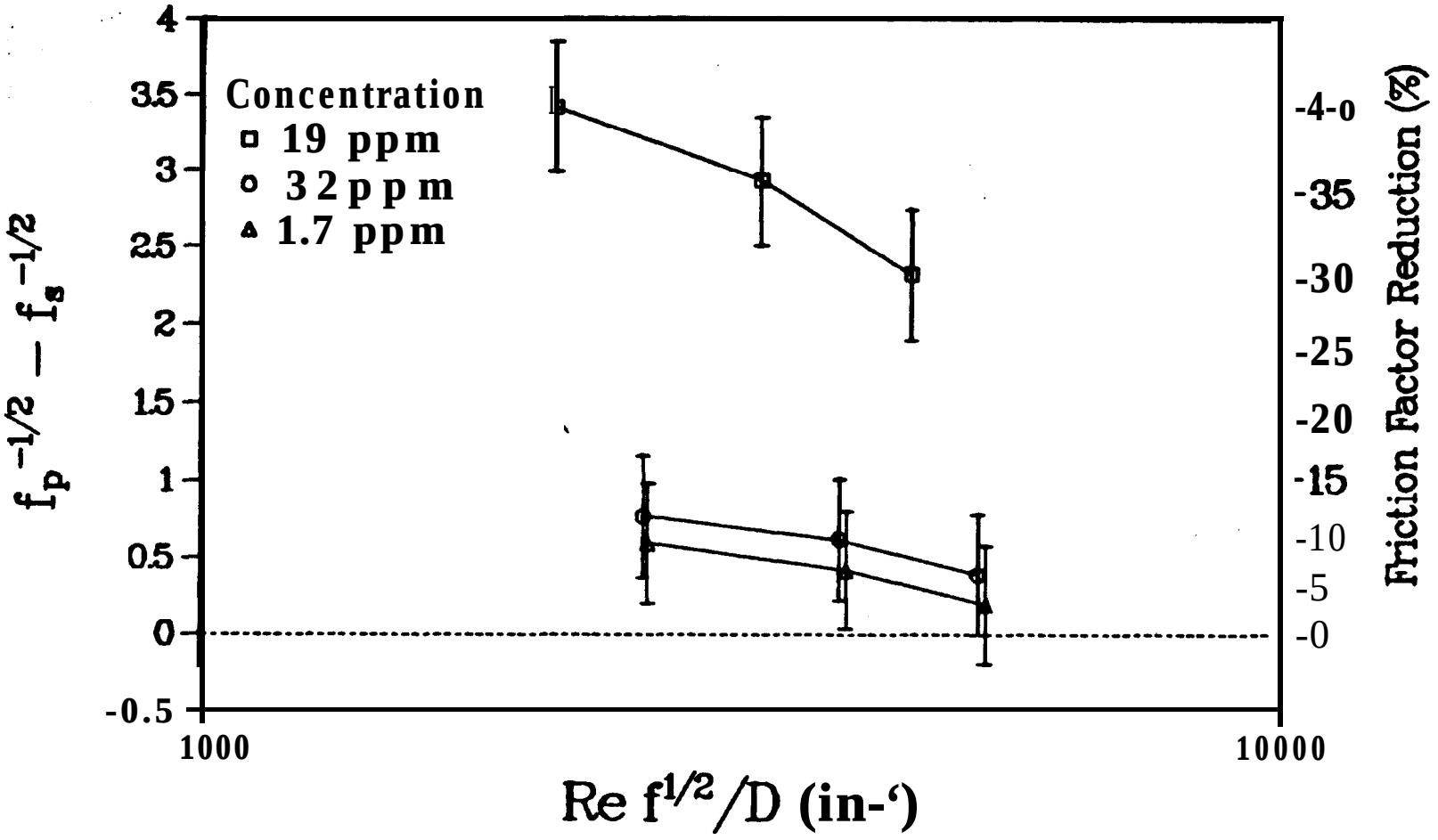

Figure 4. Relationship between Reynolds Number **and friction factor on differential** P-K **coordinates for material #2. For reference purposes an approximate nonlinear coordinate is constructed on the right hand ordinate. It shows the percentage reduction in friction factor, or, correspondingly, the percentage reduction in pressure drop at constant flow.**

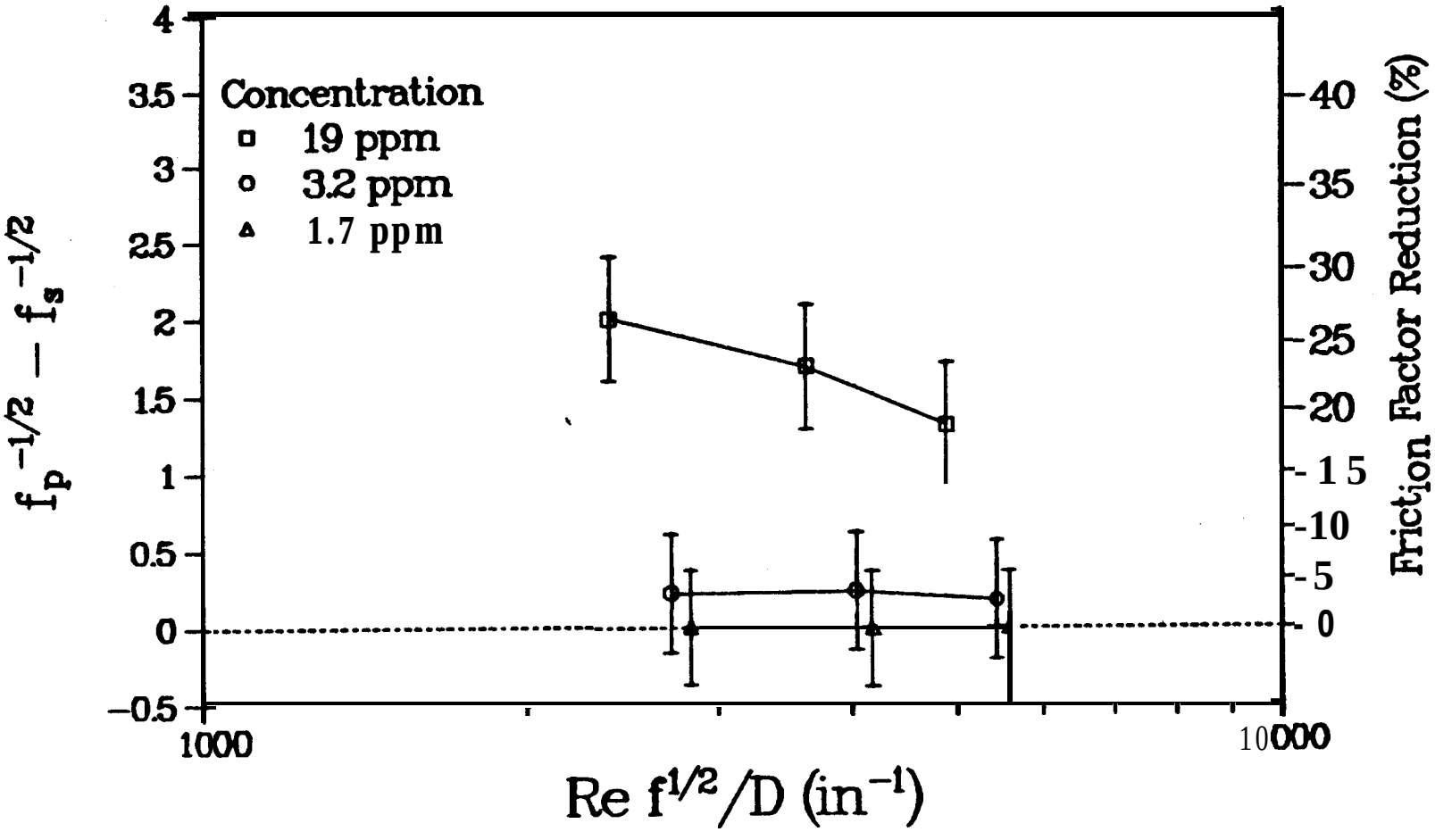

Figure 5. Relationship between Reynolds Number and friction factor on differential P-K coordinates for material #3. For reference purposes an approximate nonlinear coordinate is constructed on the right hand ordinate. It shows the percentage reduction in friction factor, or, correspondingly, the percentage reduction in pressure drop at constant flow.

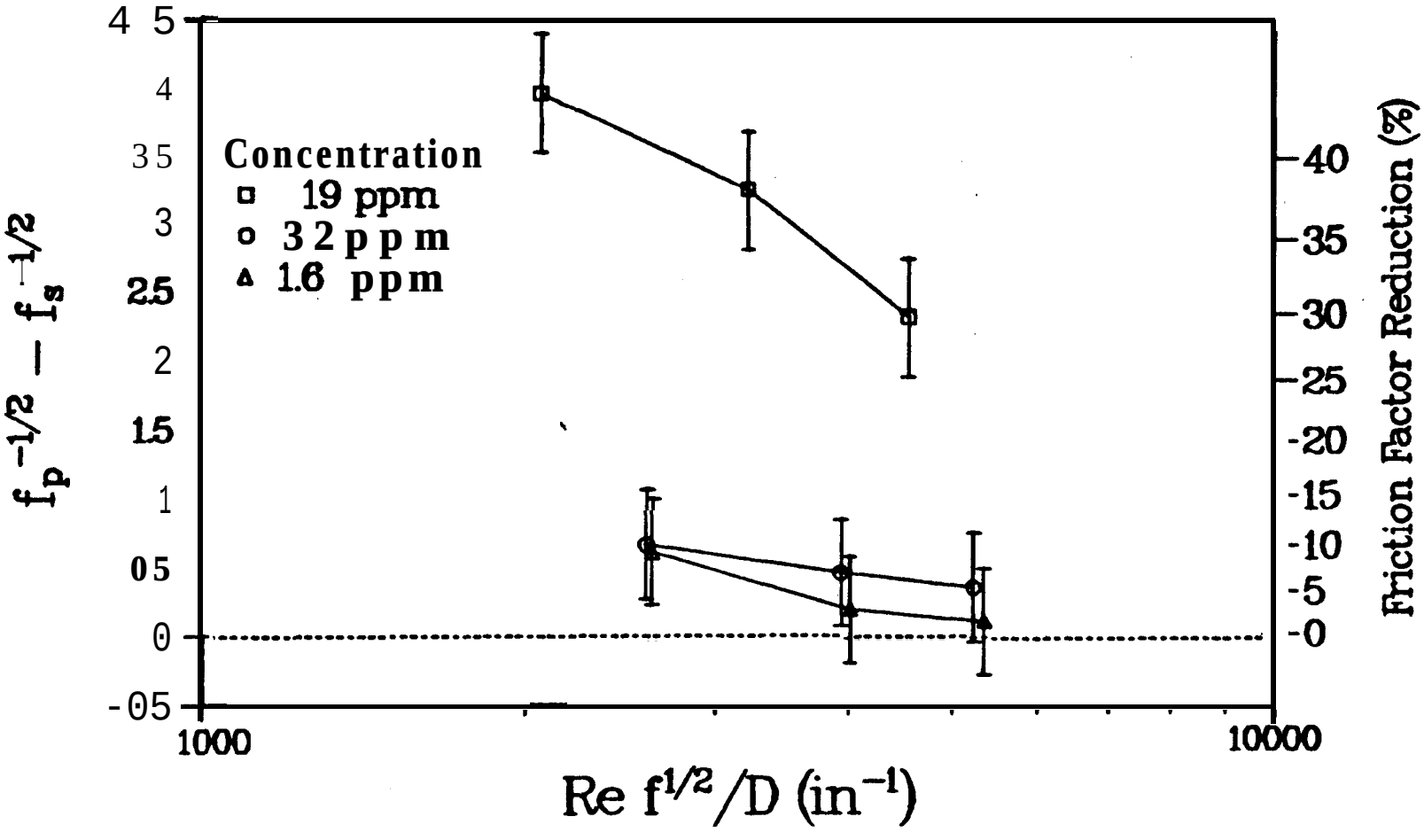

Figure 6. Relationship between Reynolds Number and friction factor on differential P-K coordinates for material #4. For reference purposes an approximate nonlinear coordinate is constructed on the right hand ordinate. It shows the percentage reduction in friction factor, or, correspondingly, the percentage reduction in pressure drop at constant flow.

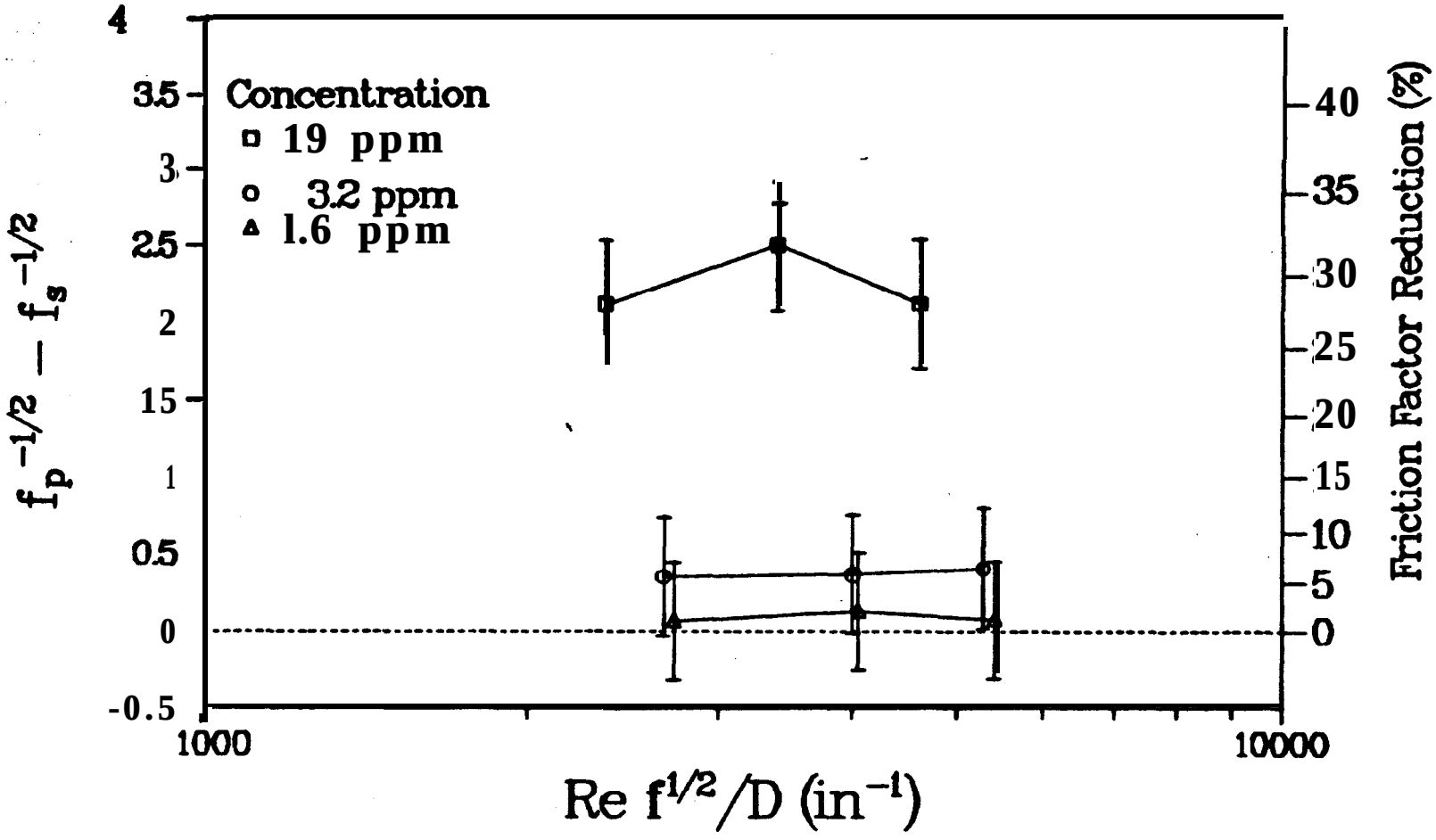

Figure 7. Relationship between Reynolds Number and friction factor on differential P-K coordinates for material #5. For reference purposes an approximate nonlinear coordinate is constructed on the right hand ordinate It shows the ercentage reduction in friction factor, or, correspondingly, he percentage reduction in pressure drop at constant flow.

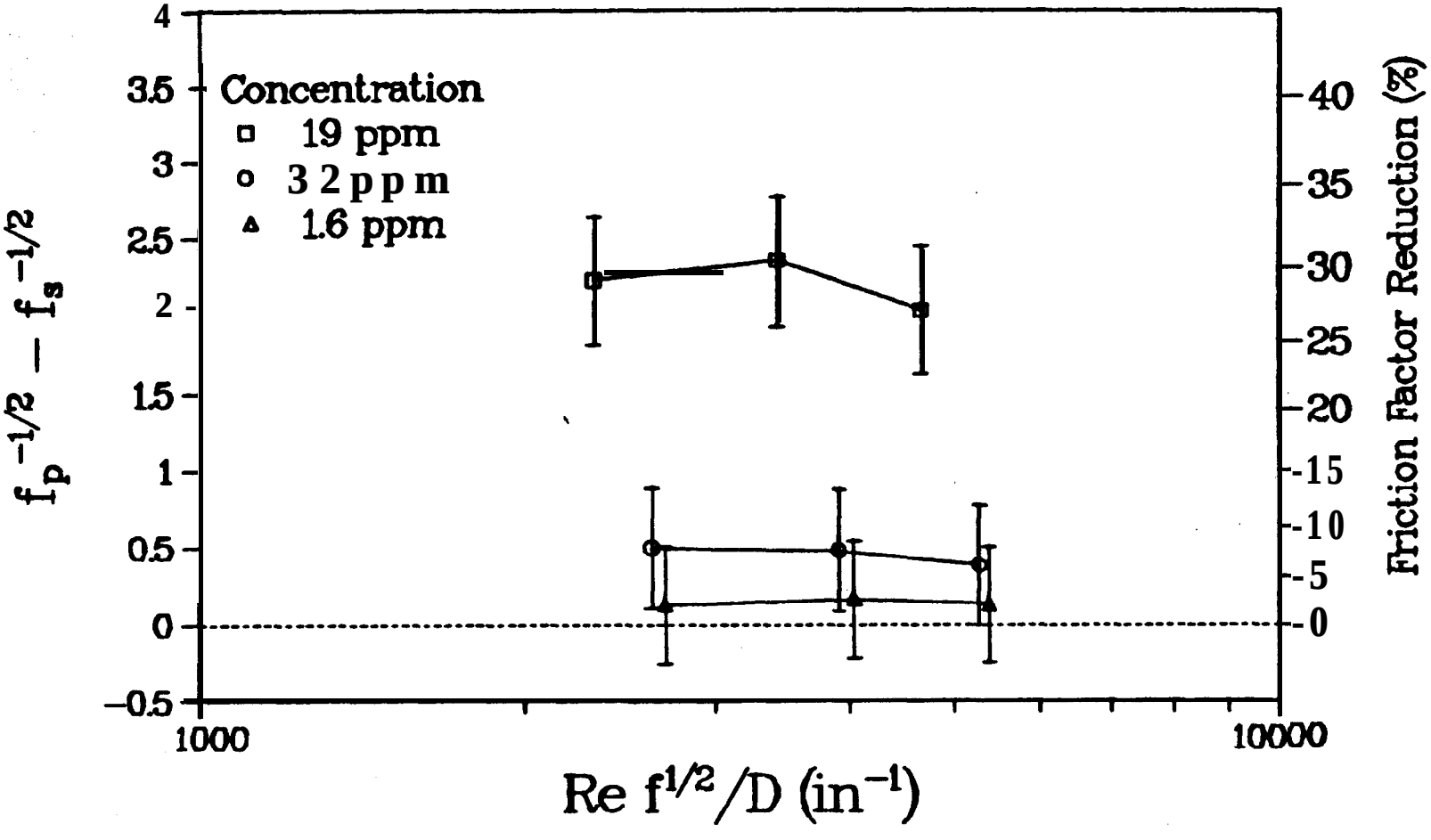

Figure 8. Relationship between Reynolds Number and friction factor on differential P-K coordinates for material #6. For reference purposes an approximate nonlinear coordinate is constructed on the right hand ordinate. It shows the percentage reduction in friction factor, or, correspondingly, the percentage reduction in pressure drop at constant flow.

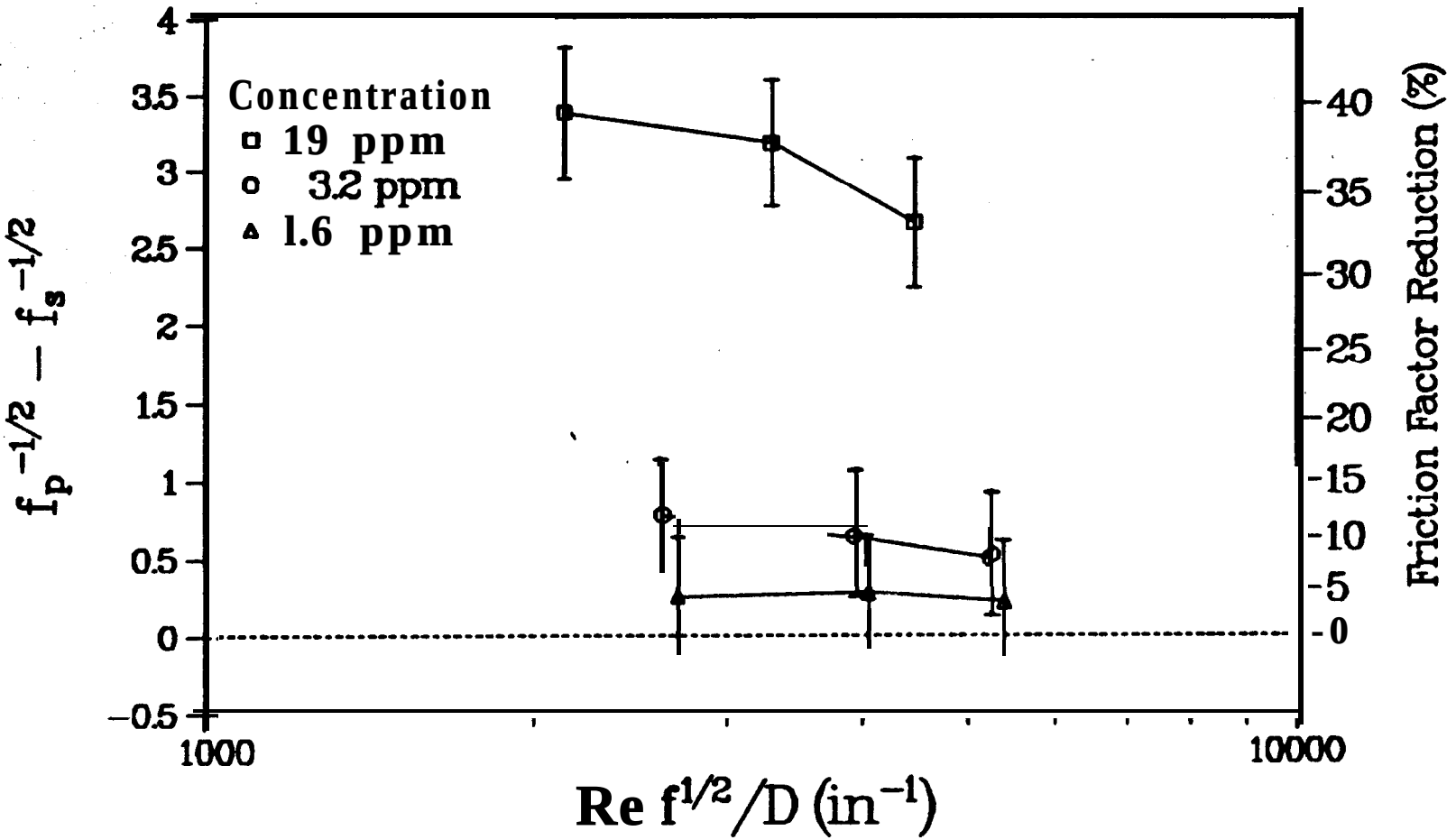

Figure 9. Relationship between Reynolds Number and friction factor on differential P-K coordinates for material #7. For reference purposes an approximate nonlinear coordinate is constructed on the right hand ordinate. It shows the percentage reduction in friction factor, or, correspondingly, the percentage reduction in pressure drop at constant flow.

the error in the flow rate increases to a maximum of 20% of the average flow rate.

ANALYSIS OF RESULTS

As may be seen in Figures 3 through 9, the performance of all DRAs increased with concentration. Material #1 (Figure 3) was a natural guar product which exhibited a small increase in performance with increased wall shear stress or, correspondingly, flow rate. The maximum reduction in friction factor observed with this material was 8.98.

Much higher performance was observed in materials #2, #3, #4, #5, #6, and #7, which are all polyacrylamide based emulsion polymers. Maximum reduction in friction factor ranged between 27%-44% for all these DRAs. Materials #2, #3, #4, #6, and #7 exhibit a general decrease in performance as the wall shear stress increases. This decrease is indicative of Region III behavior where pipeline roughness disrupts the action of the DRA. The slight increase in performance observed for materials #1 and #5 indicate that these polymers are more stable to pipeline roughness.

Materials #1 and #3 were observed to give no flow improvement at the lowest concentrations tested.

A cross comparison of all DRAs may be made at any wall shear stress or, correspondingly, any value of $(Re\sqrt{f}/d)$. Since the 36-inch brine disposal pipeline is currently operating at 850,000 BBL/day, $(Re\sqrt{f}/d)$ for this pipeline is calculated to be 3820 in^{-1}. Hence, a comparison of the ordinates of Figures 3 through 9 at this value of the abscissa allows for an estimate of the improvement available in the 36-inch pipeline, as well as a comparison of the relative performance of all DRAs.

Figure 10 gives a plot of the improvement,

$$\frac{1}{\sqrt{f_p}} - \frac{1}{\sqrt{f_s}} ,$$

at

$$\frac{Re\sqrt{f}}{d} = 3820\ in^{-1}$$

versus concentration for all of the materials. This plot is constructed on log-log coordinates since it has been previously observed [3] that flow improvement resulting from the use of DRAs

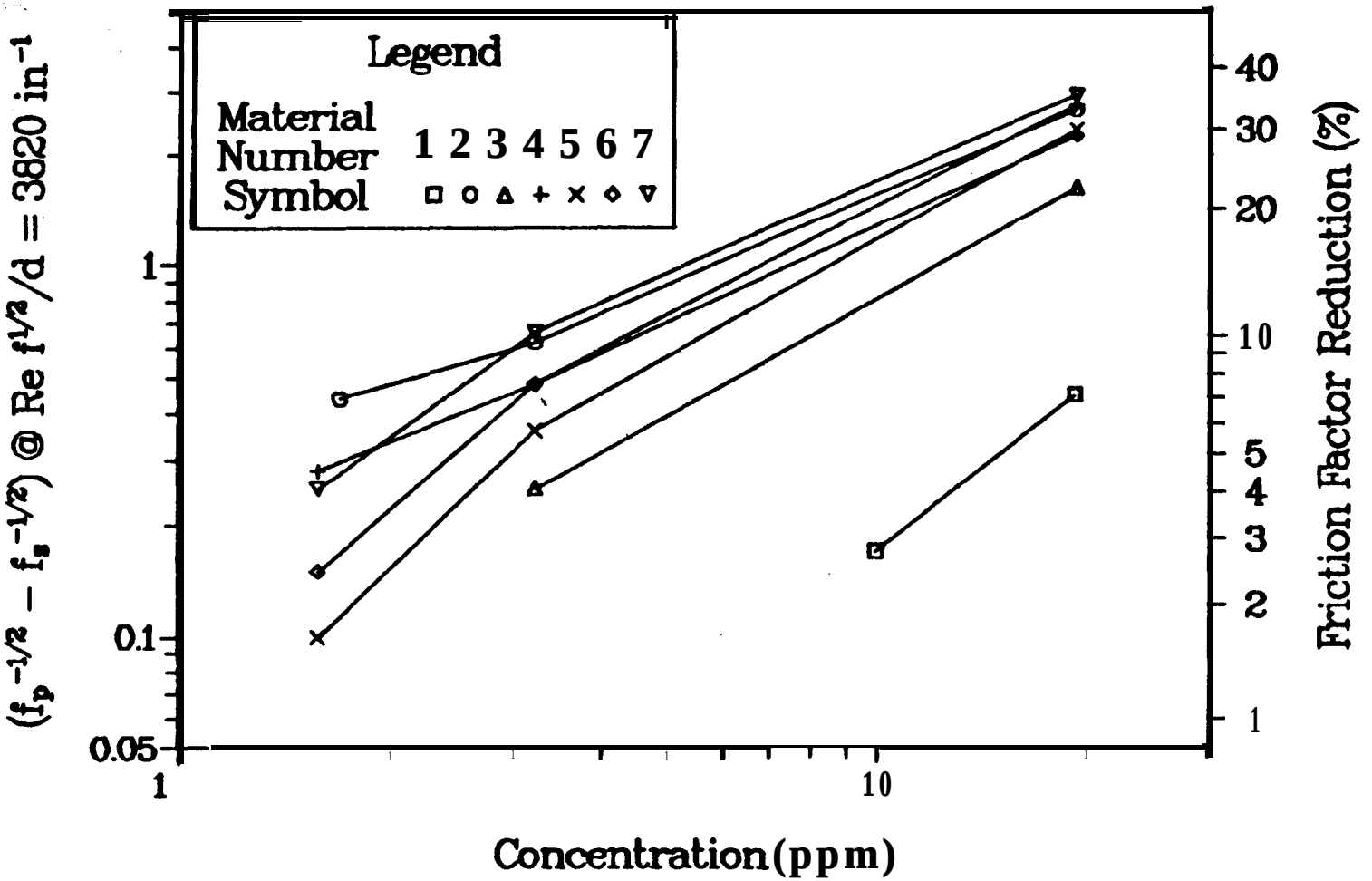

Figure 10. Plot of improvement *in* **($f_p^{-1/2} - f_s^{-1/2}$) at 36-inch diameter pipeline condition versus concentration of DRA Approximate friction** factor **reduction is shown on right ordinate.**

has a power model dependence on concentration, or

$$\left(\frac{1}{\sqrt{f_p}} - \frac{1}{\sqrt{f_s}}\right)\tau_o = m\,c^n$$

where the improvement,

$$\left(\frac{1}{\sqrt{f_p}} - \frac{1}{\sqrt{f_s}}\right)$$

is evaluated at a constant value of wall shear stress, τ_o, and c is the DRA concentration. m and n are constants to be determined for each polymer.

As seen in Figure 10, the data are approximately linear on log--log coordinates and all of the deviation from linearity is within the error tolerances shown in Figures 3 through 9. All of the polyacrylamide **DRAs, #2** through **#7,** have slopes of approximately 0.9 while the guar DRA, **#1,** has a slope of approximately 1.5. For this application a smaller slope is preferred since this results in higher drag reduction at **lower** concentration and consequently lower cost. Only minor differences were observed among the polyacrylamide **DRAs.** Materials **#2** and **#7** were the best performers at 3 ppm, followed closely by materials **#4** and **#6.** At 19 ppm **#4** performed as well as **#2,** and **#5** performed as well as **#6.** Material **#3** paralleled the performance of **#5** but was slightly below it. Despite these minor differences, all of the polyacrylamide **DRAs** performed comparably and within error tolerances of one another. The guar DRA, **#1,** was significantly below all of the **polyacrylamides.**

Values of m and n are tabulated for all of the **DRAs** in Table 8. These values are presented here for completeness and ease of comparison. Both maximum and minimum values of m are **presented** to reflect the uncertainty of the data.

All of the materials were found to have significant fluid friction reducing properties which, based on technical considerations alone, make them **likely** candidates for commercial application as drag reducing agents.

Table 8.
Concentration Dependence of DRAs in Terms of Power Law Model

Material	n	m	Error Range on m
1	1.48	0.0056	.00 < m < .13
2	0.81	0.24	.05 < m < .51
3	1.05	0.073	.00 < m < .31
4	0.97	0.16	.01 < m < .39
5	1.05	0.11	.00 < m < .33
6	0.87	0.17	.01 < m < .43
7	0.83	0.25	.05 < m < .53

CONCLUSIONS

1. An evaluation of seven drag reducing agents was performed in a 3-inch pipeline at West Hackberry, Louisiana. The seven DRAs represent two distinct classes of materials: guar and polyacrylamide. Some performance differences between the two classes of materials were observed. The polyacrylamide DRAs had a higher level of activity than the guar DRA but demonstrated a susceptibility to pipe roughness that the guar did not. The six polyacrylamide DRAs showed maximum friction factor reductions at 19 ppm between 27% and 44%. The maximum friction factor reduction for the guar DRA was 9%. The flow improvements may all be considered significant from the standpoint of commercial application.

2. The performance of each DRA was fit to a power law model in concentration. The performances of the polyacrylamides were all proportional to approximately the 0.9 power of concentration while that of the guar was proportional to the concentration to the 1.5 power.

3 By testing at a wall shear stress which was equivalent to that observed in the 36-inch brine disposal pipeline at West Hackberry, the results of this 3-inch pipeline test provide estimates of the results expected in the 36-inch pipeline. However, the much larger roughness of the large diameter pipeline may reduce the improvements observed here.

4 A standard error analysis was used to estimate an upper bound on the measurement error for these experiments. However, the procedure of repeating each baseline pressure differential measurement before any DRA addition should have minimized the real experimental error.

REFERENCES

1. Bowles, E. B., Jr., "Brine/Polymer Mixture Drag Reduction Characteristics," Final Report on Contract 47-2033, SwRI Project No 06-7664, October, 1983.

2. Hinkebein, T. E., "An Analysis of Drag Reducing Agents For Use at the Strategic Petroleum Reserve Site at West Hackberry, Louisiana," SAND85-0045, May, 1985.

3. Virk, P. S., "Drag Reduction Fundamentals," A.I.Ch.E.J., 21, 625, 1975.

4. Virk, P. S., "Drag Reduction in Rough Pipes," J. Fluid Mech., 45. 225, 3971.

Distribution:

US Department of Energy
Strategic Petroleum Reserve PMO
Attn: E. E. Chapple, PR-632 (8)
TDCS (2)
900 Commerce Road East
New Orleans, LA 70123

US Department of Energy (2)
Strategic Petroleum Reserve
Attn: D. Johnson
D. Smith
1000 Independence Ave., SW
Washington, D.C. 20585

US Department of Energy (1)
Oak Ridge Operations Office
Attn: J. Milloway
P.O. Box E
Oak Ridge, TN 37831

Aerospace Corporation (2)
Attn: R. Merkle
800 Commerce Road East, Suite 300
New Orleans, LA 70123

Walk Haydel & Associates (1)
Attn: J. Mayes
600 Carondelet St.
New Orleans, LA 70130

PB/KBB (4)
Attn: H. Lombard
850 S. Clearview Parkway
New Orleans, LA 70123

Boeing Petroleum Services (2)
Attn: K. Mills
850 South Clearview Parkway
New Orleans. LA 70123

Solution Mining Research Institute
Attn: Howard Fiedelman
812 Muriel Street
Woodstock, IL 60098

Southwest Research Institute (1)
Attn: E. B. Bowles, Jr.
6220 Culebra Rd.
San Antonio, TX 78284

U.S. Department of Energy
Attn: J. Hale
P. 0. Box E
Oak Ridge, TN 37830

6200 V. L. Dugan
6250 B. W. Marshall
6257 J. K. Linn (10)
6257 R. R. Beasley
6257 K. L. Biringer
6257 D. K. Buchanan
6257 K. L. Goin
6257 C. A. Searls
6257 J. L. Todd, Jr.
6257 T. E. Hinkebein (10)
3141 S. Landenburger (5)
3151 W. L. Garner (3)
3154-1 c. H. Dalin (28) for Unlimited Distribution